Report

A highly immunogenic live-attenuated vaccine candidate prevents SARS-CoV-2 infection and transmission in hamsters

Xiao-Feng Li,[1,5] Zhen Cui,[2,5] Hang Fan,[1,5] Qi Chen,[1,5] Lei Cao,[2,5] Hong-Ying Qiu,[1] Na-Na Zhang,[1,3] Yan-Peng Xu,[1] Rong-Rong Zhang,[1] Chao Zhou,[1] Qing Ye,[1] Yong-Qiang Deng,[1] Yan Guo,[1] Si Qin,[1] Kaiyue Fan,[2] Lei Wang,[2] Zijing Jia,[2] Yujun Cui,[1,*] Xiangxi Wang,[2,*] and Cheng-Feng Qin[1,4,*]

*Correspondence: cuiyujun.new@gmail.com (Y.C.); xiangxi@ibp.ac.cn (X.W.); qincf@bmi.ac.cn (C.-F.Q.)

Received: November 11, 2021; Accepted: February 28, 2022; Published Online: March 2, 2022; https://doi.org/10.1016/j.xinn.2022.100221

GRAPHICAL ABSTRACT

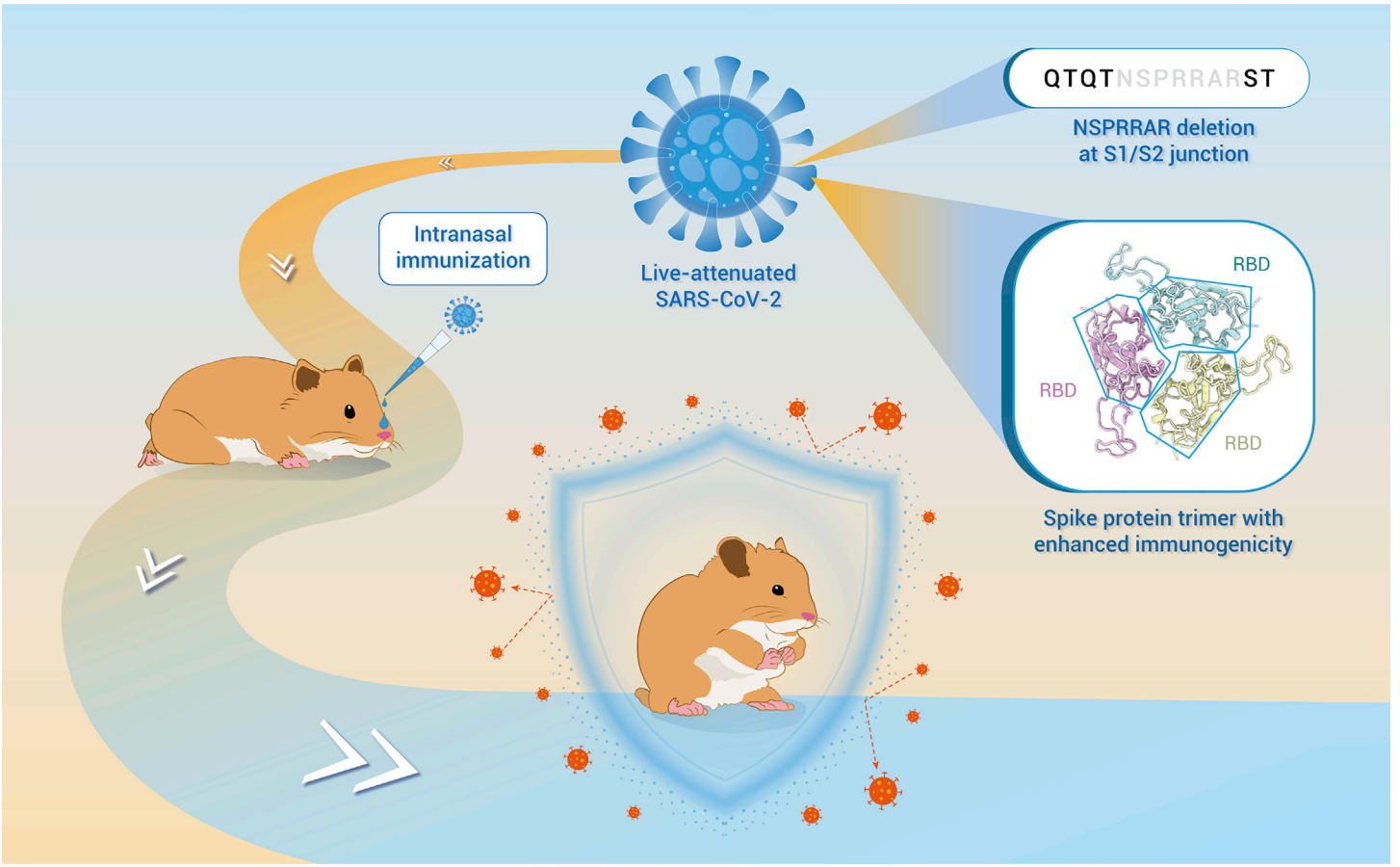

PUBLIC SUMMARY

- Passaging of a protype SARS-CoV-2 in Vero cells generates a live-attenuated VAS5
- A 7 amino acids deletion of the S protein contributes to the attenuated phenotype
- VAS5 immunization prevents SARS-CoV-2 infection and transmission in Syrian hamsters
- The VAS5 S protein forms a locked prefusion conformation with enhanced immunogenicity

Report

A highly immunogenic live-attenuated vaccine candidate prevents SARS-CoV-2 infection and transmission in hamsters

Xiao-Feng Li,[1,5] Zhen Cui,[2,5] Hang Fan,[1,5] Qi Chen,[1,5] Lei Cao,[2,5] Hong-Ying Qiu,[1] Na-Na Zhang,[1,3] Yan-Peng Xu,[1] Rong-Rong Zhang,[1] Chao Zhou,[1] Qing Ye,[1] Yong-Qiang Deng,[1] Yan Guo,[1] Si Qin,[1] Kaiyue Fan,[2] Lei Wang,[2] Zijing Jia,[2] Yujun Cui,[1,*] Xiangxi Wang,[2,*] and Cheng-Feng Qin[1,4,*]

[1]Department of Virology, State Key Laboratory of Pathogen and Biosecurity, Beijing Institute of Microbiology and Epidemiology, Academy of Military Medical Sciences, Beijing 100071, China

[2]CAS Key Laboratory of Infection and Immunity, National Laboratory of Macromolecules, Institute of Biophysics, Chinese Academy of Sciences, Beijing 100101, China

[3]School of Medicine, Tsinghua University, Beijing 100084, China

[4]Research Unit of Discovery and Tracing of Natural Focus Diseases, Chinese Academy of Medical Sciences, Beijing 100071, China

[5]These authors contributed equally

*Correspondence: cuiyujun.new@gmail.com (Y.C.); xiangxi@ibp.ac.cn (X.W.); qincf@bmi.ac.cn (C.-F.Q.)

Received: November 11, 2021; Accepted: February 28, 2022; Published Online: March 2, 2022; https://doi.org/10.1016/j.xinn.2022.100221

Citation: Li X.-F., Cui Z., Fan H., et al., (2022). A highly immunogenic live-attenuated vaccine candidate prevents SARS-CoV-2 infection and transmission in hamsters. The Innovation **3(2)**, 100221.

The highly pathogenic and readily transmissible SARS-CoV-2 has caused a global coronavirus pandemic, urgently requiring effective countermeasures against its rapid expansion. All available vaccine platforms are being used to generate safe and effective COVID-19 vaccines. Here, we generated a live-attenuated candidate vaccine strain by serial passaging of a SARS-CoV-2 clinical isolate in Vero cells. Deep sequencing revealed the dynamic adaptation of SARS-CoV-2 in Vero cells, resulting in a stable clone with a deletion of seven amino acids (N_{679}SPRRAR$_{685}$) at the S1/S2 junction of the S protein (named VAS5). VAS5 showed significant attenuation of replication in multiple human cell lines, human airway epithelium organoids, and hACE2 mice. Viral fitness competition assays demonstrated that VAS5 showed specific tropism to Vero cells but decreased fitness in human cells compared with the parental virus. More importantly, a single intranasal injection of VAS5 elicited a high level of neutralizing antibodies and prevented SARS-CoV-2 infection in mice as well as close-contact transmission in golden Syrian hamsters. Structural and biochemical analysis revealed a stable and locked prefusion conformation of the S trimer of VAS5, which most resembles SARS-CoV-2-3Q-2P, an advanced vaccine immunogen (NVAX-CoV2373). Further systematic antigenic profiling and immunogenicity validation confirmed that the VAS5 S trimer presents an enhanced antigenic mimic of the wild-type S trimer. Our results not only provide a potent live-attenuated vaccine candidate against COVID-19 but also clarify the molecular and structural basis for the highly attenuated and super immunogenic phenotype of VAS5.

INTRODUCTION

Severe acute respiratory syndrome coronavirus 2 (SARS-CoV-2) is a new betacoronavirus that includes two highly pathogenic coronaviruses, SARS-CoV and Middle East respiratory syndrome coronavirus (MERS-CoV).[1–3] SARS-CoV-2 infection leads to coronavirus disease 2019 (COVID-19), characterized by a spectrum of etiological findings ranging from asymptomatic disease to mild upper respiratory tract infection symptoms.[4] More severe COVID-19 cases develop acute respiratory distress syndrome and acute lung injury, leading to morbidity and mortality caused by damage to the alveolar lumen.[5,6] SARS-CoV-2 can be transmitted by direct human-to-human respiratory droplet contact and aerosols, and has high human-to-human transmissibility, with an estimated basic reproduction number (R0) ranging from 1.4 to 8.0.[7–9] Due to being highly pathogenic and readily transmissible, SARS-CoV-2 has caused a global COVID-19 pandemic with more than 400 million confirmed cases and more than 5.7 million deaths worldwide as of January 2022.

The spike (S) protein of SARS-CoV-2 is a homotrimeric membrane protein responsible for virus entry into host cells. The S protein is composed of two functional subunits, S1 and S2, which are involved in binding to human angiotensin-converting enzyme 2 (hACE2) at the cell membrane and the fusion between virus and cellular membranes, respectively.[2,10,11] Upon virus attachment to host receptors, the S protein undergoes a large conformational rearrangement to allow host proteases to cleave at one or more positions (termed the S1/S2 and S2′ sites). Priming of the S protein by host proteases is a crucial factor modulating the tropism and pathogenicity of coronaviruses.[12] The SARS-CoV-2 S protein harbors a unique insertion of a polybasic furin-like cleavage site (RRAR) positioned upstream of the S1/S2 junction, which is absent in SARS-CoV and the highly related bat coronavirus RaTG13.[13–15] Similar cleavage sites have been associated with increased pathogenicity in other viruses.[16–18] Due to the near-ubiquitous distribution of furin-like proteases, the acquisition of this cleavage site is supposed to provide a gain-of-function to SARS-CoV-2 for efficient infection and spreading in the human population.[19]

The function of this notable cleavage site in SARS-CoV-2 remains largely unknown. In fact, insertion of a furin-like cleavage site at the S1/S2 site enhanced cell-cell fusion of SARS-CoV.[20] Hoffmann et al. reported that a highly cleavable S1/S2 site is essential for S protein-mediated cell-cell fusion and entry into human lung cells.[21] Recently, SARS-CoV-2 variants with deletions at the S1/S2 site have been detected in clinical samples.[22–25] A set of previous findings also suggests that these variants can be selected following passaging in Vero cells.[23,24,26,27] However, the biological function and the structural basis for these specific deletions remain unknown. In addition, a panel of vaccines, including mRNA, viral vector-based, inactivated vaccines, and protein subunit vaccines, have been approved for clinical usage.[28–32] However, no live-attenuated vaccines against SARS-CoV-2 have been approved for human use.

Herein, we report the generation of a live-attenuated strain of SARS-CoV-2 (termed VAS5) bearing a seven-amino-acid (aa) deletion upstream of the S1/S2 junction in the S protein by serial passaging of a protype strain of SARS-CoV-2 in Vero cells. The promising profiles of VAS5, including ideal safety, genetic stability, immunogenicity, and protection efficacy in hamsters, support its further development in human trials. More importantly, combining deep sequencing and cryoelectron microscopy (cryo-EM) analysis, we reveal the molecular and structural basis for the highly attenuated and super immunogenic phenotype of VAS5.

RESULTS

Serial passaging of SARS-CoV-2 in Vero cells leads to a specific deletion in the S protein

During the preparation of working stocks of the inactivated SARS-CoV-2 vaccine in Vero cells,[33] we detected a seven-aa deletion (N_{679}SPRRAR$_{685}$, Δ679-685) upstream of the S1/S2 junction in the S protein by Sanger sequencing (Figure 1A). To further profile the dynamic process of viral adaptation in Vero cells, full-length genomes of viruses from passage 1 (P1) to P5 were determined by deep sequencing. Large panels of variants with deletions of different lengths and positions were detected among the different SARS-CoV-2 passages (Figure 1B). The Δ679-685 variant was first detected at P3 and rapidly increased at P4, finally becoming the predominant variant at P5 (99.119%). Notably, the P1 and P2 viruses contained few variants, and only a two-aa deletion ($Q_{675}T_{676}$, Δ675-676) and a five-aa deletion (Q_{675}TQTN_{679}, Δ675-679) accounted for 0.020% and 0.129%, respectively. Two variants with a six-aa deletion (P_{681}RRARS$_{686}$, Δ681-686) or another seven-aa deletion (S_{680}PRRARS$_{686}$, Δ680-686) emerged in the P3 virus and were maintained in the P4 virus but disappeared in the P5 virus. Other variants carrying different deletions or substitutions were also detected during passaging (Figures 1B and S1A). Sanger sequencing of P5 further passaged in Vero cells confirmed its good genetic

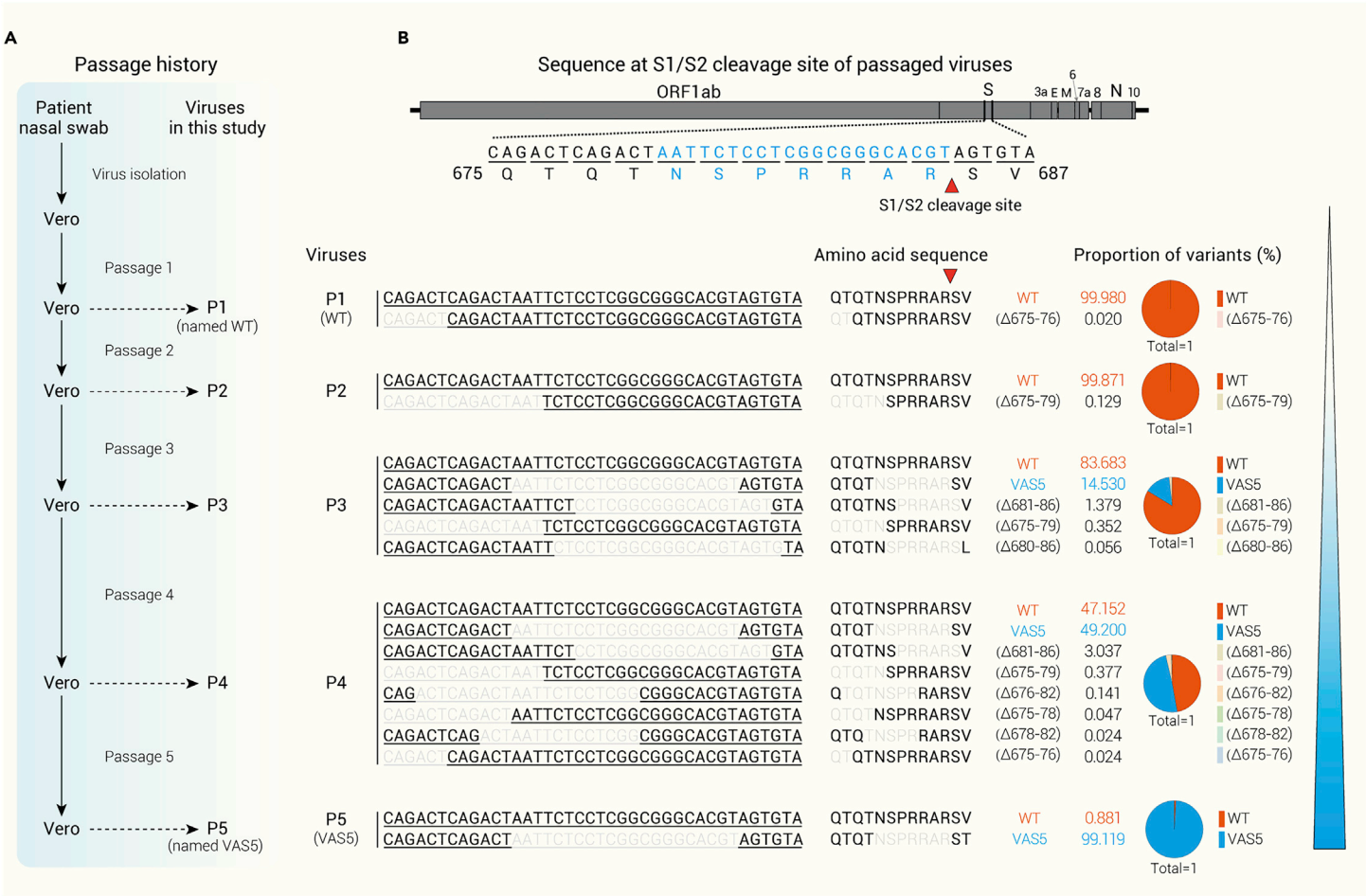

Figure 1. Profile of nucleotide and amino acid sequences located at the S1/S2 cleavage site of the S protein of variants during passaging of SARS-CoV-2 in Vero cells
(A) Schematic diagram of the passage history of Vero-adapted SARS-CoV-2. SARS-CoV-2 isolated from a COVID-19 patient was passaged in Vero cells five times. The virus at passage 1 was named WT, and the virus at passage 5 with a deletion of seven-aa in the S protein was named VAS5. (B) Profiles of the nucleotide sequence and amino acid sequence located at the S1/S2 cleavage site in the S protein of variants during passaging and adaptation in Vero cells.

stability (Figure S1B). The P5 virus bearing the seven-aa deletion (Δ679-685) was named VAS5 and subjected to further testing.

VAS5 shows reduced infectivity and fitness in human airway epithelium organoids

To characterize the *in vitro* phenotypes of VAS5, a set of cells, including Vero, Huh7, and Caco-2 cells, were infected with VAS5 or its parental virus (wild type [WT]) and subjected to RT-qPCR and immunofluorescence staining. VAS5 showed replication capability similar to WT in Vero cells, while no increase in viral RNAs or viral protein expression of VAS5 was detected in either Huh7 or Caco-2 cells (Figures 2A and 2B). In contrast, the WT virus replicated well in all three types of cells. These results suggest that VAS5 lost its ability to infect human cells.

We then determined the infectivity of VAS5 in human trachea and lung epithelium organoids cultured at the air-liquid interface in comparison with WT. A large number of SARS-CoV-2 S protein-positive cells in both tracheal and lung organoids were detected at 48 h following WT infection, while only a few positive cells were detected in VAS5-infected organoids (Figures 2C and 2D). Similarly, the viral RNA loads in the VAS5-infected organoids were much lower than those in the WT-infected organoids (Figures 2C and 2D).

Furthermore, to explore the potential mechanism of restricted replication in the human airway epithelium, we performed a standard viral fitness competition assay in both Vero cells and the human bronchus epithelium (Figure 2E). VAS5 increased to 80% of the total reads following 3 days of competition culture in Vero cells (Figure 2F). In contrast, VAS5 decreased significantly to 5% of the total reads following 3 days of competition in human tracheal epithelium organoids (Figure 2G). These results demonstrate that, compared with WT, VAS5 acquired a fitness advantage in Vero cells but had comparatively less replicative fitness in the human airway epithelium.

VAS5 is highly attenuated and immunogenic in mice

We further characterized the infection and pathogenic features of VAS5 in hACE2 mice. Groups of hACE2 mice were intranasally (i.n.) inoculated with equal doses of VAS5 and WT. As expected, WT inoculation resulted in robust viral RNA replication in mouse lungs, as evidenced by RT-qPCR and *in situ* hybridization (ISH) (Figures S2A and S2B), with notable lung damage characterized by a mildly thickened septa (Figure S2B). While the viral RNA loads in the lungs from VAS5-infected mice were significantly lower (up to 10-fold reduction) than those from the WT-infected mice (Figure S2A), only marginal RNAs were detected in lung sections from VAS5-infected mice (Figure S2B). No lung pathological changes were induced by the VAS5 challenge (Figure S2B). These results clearly demonstrate that the *in vivo* replication and pathological outcome of VAS5 are highly attenuated in hACE2 mice.

As VAS5 contained a seven-aa deletion in the S protein, we further sought to determine whether VAS5 immunization conferred protection against SARS-CoV-2. Inactivated VAS5 was prepared as previously described.[33] Groups of female BALB/c mice were intramuscularly (i.m.) immunized at days 0 and 14 with two doses of 1.25 μg or 2.5 μg of inactivated VAS5 or PBS. Forty days after the initial immunization, mice were inoculated i.n. with a mouse-adapted SARS-CoV-2 strain, MASCp6, as previously described.[34] Viral RNA loads in the lungs and tracheas were determined by RT-qPCR. As expected, significantly decreased viral RNA was detected in the indicated tissues of inactivated VAS5-immunized mice compared with that of the PBS group (Figure S2C). The immunostaining assay showed an abundance of cells positive for SARS-CoV-2 S protein expression in lung sections of mice in the PBS group, whereas significantly fewer positive cells were detected in the lungs of VAS5-immunized mice (Figure S2D). These data indicate good immune protection provided by inactivated VAS5 against SARS-CoV-2 challenge in mice. Finally, we further

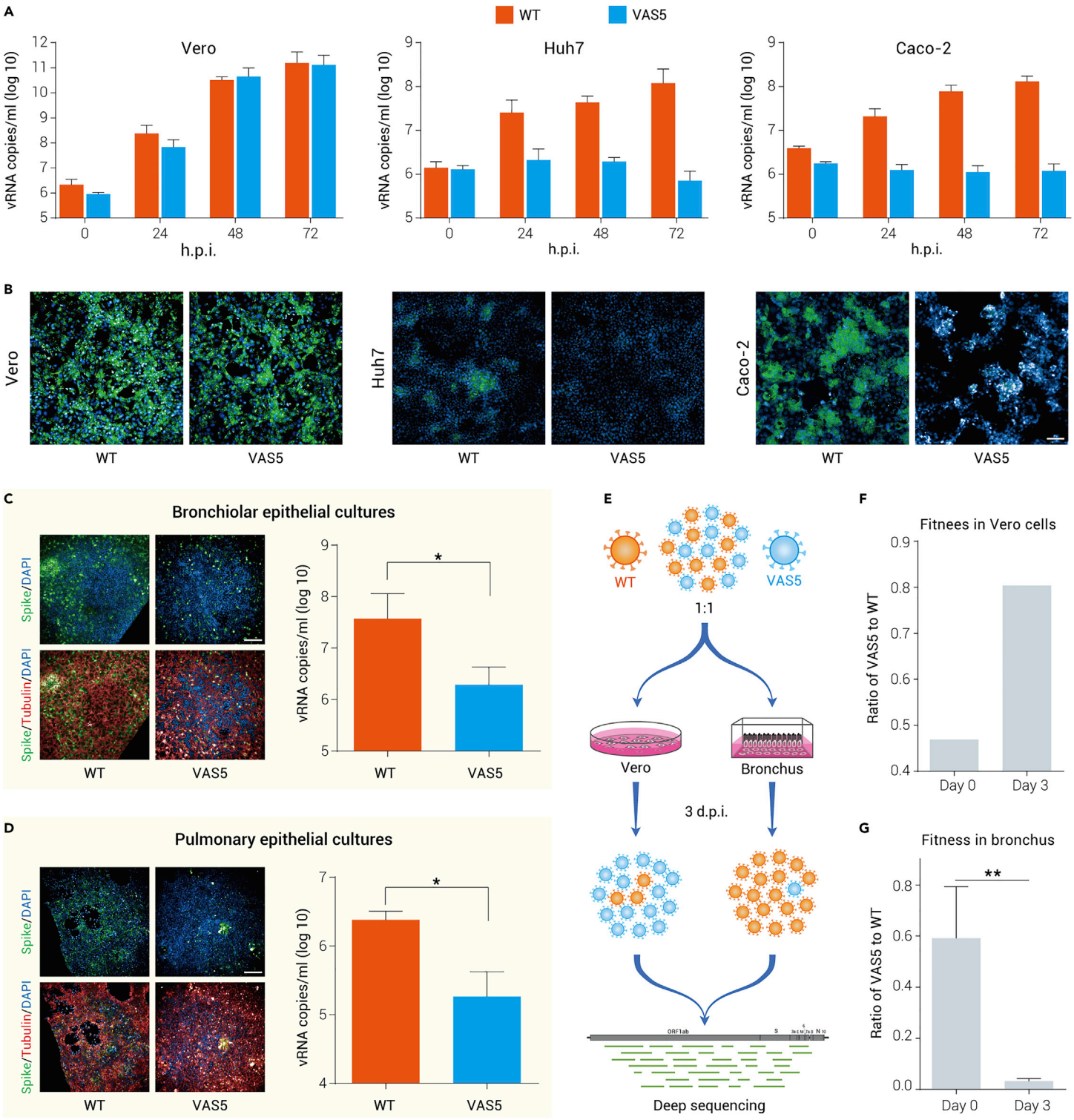

Figure 2. VAS5 virus exhibits less replicative fitness in human cell lines and human respiratory epithelial ALI culture (A) Growth curves of WT and VAS5 in Vero, Huh7, and Caco-2 cells. Viruses were inoculated into cells at an MOI of 0.01. Viral RNA was detected at the indicated times using RT-qPCR. (B) Immunofluorescence assay (IFA) of viral proteins expressed in the indicated cells following virus infection. Cells were infected with WT or VAS5 at an MOI of 0.01. Viral S proteins were detected at 48 hours post infection (h.p.i.) by IFA using an S protein-specific antibody. Scale bar, 100 μm. (C) Human respiratory epithelial ALI cultures, including the bronchus and lung, were infected with WT or VAS5, and viral RNA in the topical secretions was detected at 48 h.p.i. using RT-qPCR. Data are shown as the mean ± SEM (*$p < 0.05$). Scale bar, 200 μm. (D) High-content imaging of the bronchus and lung infected with WT or VAS5 at 48 h.p.i. Data are shown as the mean ± SEM (*$p < 0.05$). Scale bar, 200 μm. (E) Schematic diagram of the fitness assay. (F and G) Fitness of WT and VAS5 in Vero cells (F) and the human respiratory epithelial ALI bronchus (G). Equal amounts of WT and VAS5 were pooled and inoculated into Vero cells or the bronchus. The viral genome was determined at 3 days p.i. by deep sequencing. Data are shown as the mean ± SEM (**$p < 0.01$).

investigated the immunogenicity of VAS5 and WT S trimers in rats. Wistar rats were immunized twice via the intramuscular route with VAS5 or WT S trimers (5 μg per dose) mixed with alum adjuvant or placebo (PBS + alum) at days 0 and 14 (n = 10) (Figure S2E). SARS-CoV-2-specific immunoglobulin (Ig)G antibody emerged at week 2 and rose up to an half maximal effective concentration (EC_{50}) of ~8,600,000 by week 3 in the VAS5 S trimer-vaccinated group, whose titer was ~2-fold higher than that of serum from the WT S trimer-immunized group at week 2 (Figure S2E). These results, coupled with the structural and immunogenic analysis, clearly support the further development of VAS5 as a potent vaccine candidate.

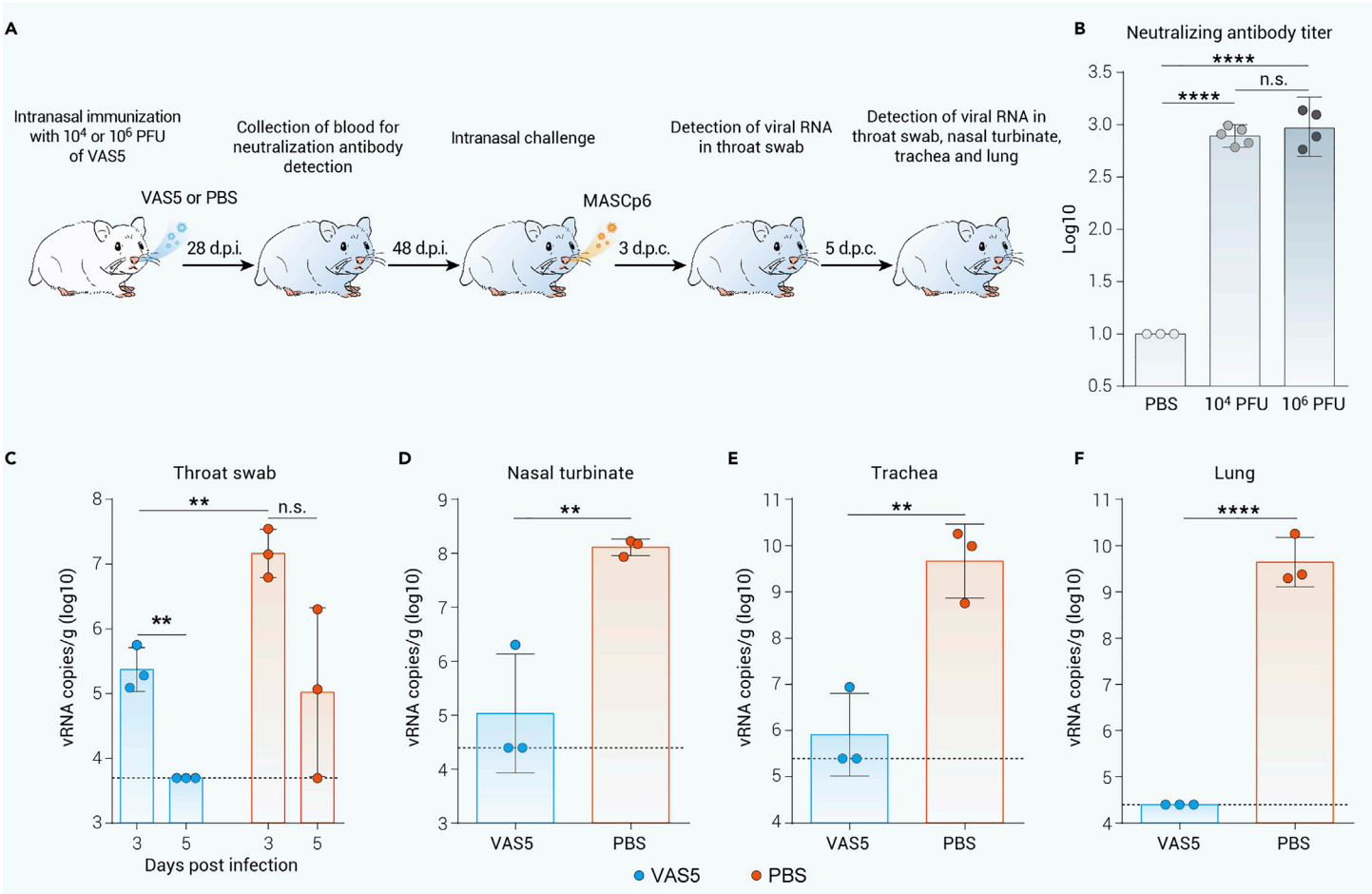

Figure 3. Live-attenuated VAS5 virus provides protection against SARS-CoV-2 challenge in hamsters (A) Study design of the prevention of contact transmission of SARS-CoV-2 in hamsters. Female hamsters were i.n. immunized with the indicated doses of live VAS5 or PBS. (B) Four weeks post-immunization, blood was collected for the detection of neutralizing antibodies against the WT virus. (C) Forty-eight days post-immunization, the animals were i.n. challenged with MASCp6. Viral RNA in throat swabs was detected using RT–qPCR at Days 3 and 5 post challenge. (D–F) The indicated tissues were also collected 5 days after challenge for detection of viral loads using RT-qPCR: (D) nasal turbinate; (E) trachea; (F) lung. Data are shown as the mean ± SEM. Statistics were determined by multiple t tests. d.p.c., days post contact; d.p.i., days post infection; n.s., not significant; **p < 0.01; ****p < 0.0001).

A single immunization with VAS5 prevents SARS-CoV-2 infection and transmission in hamsters

The immunogenicity and protection of VAS5 were further determined in the well-established golden Syrian model (Figure 3A).[35,36] A single immunization with either low or high doses of VAS5 induced high levels of neutralizing antibody (geometric mean titer [GMT] = 776 and 927, respectively) against SARS-CoV-2 (Figure 3B). Then, three animals from the low-dose group were i.n. challenged with MASCp6 on day 48 post-immunization. At day 3 post-challenge, viral RNA loads were significantly reduced in the throat swabs of VAS5-immunized animals compared with those of PBS-immunized animals (Figure 3C). Strikingly, viral RNAs were not detected in the throat swabs of all VAS5-immunized animals at day 5 post-challenge, while two of three animals immunized with PBS maintained high levels of viral RNA (Figure 3C). At day 5 post-challenge, high levels of viral RNA were detected in the nasal turbinate, trachea, and lung of all PBS-immunized animals (Figures 3D–3F), while only one of three VAS5-immunized animals sustained low levels of viral RNA in the nasal turbinate and trachea (Figures 3D and 3E). Notably, viral RNA was completely cleared in the lungs of all VAS5-immunized animals (Figure 3F).

Further we examined whether VAS5 immunization prevented close-contact transmission of SARS-CoV-2 in the established hamster model.[35] Three VAS5-immunized hamsters were i.n. challenged with MASCp6. One day post-challenge, each SARS-CoV-2-challenged hamster was transferred to a new cage, with each cage containing one naive hamster as the close contact (Figure 4A). Viral RNA present in throat swabs was determined using RT-qPCR at days 3 and 5 post close contact. High levels of viral RNA were detected in the throat swabs of native hamsters in contact with challenged hamsters immunized with PBS at days 3 and 5 post contact (Figure 4B). At day 5 post contact, all three native hamsters harbored extremely high levels of viral RNA in the indicated tissue samples (Figures 4C–4E). In contrast, very low levels of viral RNA were detected in throat swabs of native hamsters in contact with challenged animals immunized with VAS5 (Figure 4B), and no viable SARS-CoV-2 virus was isolated in the throat swab. Strikingly, at day 5 post contact, no viral RNA was detectable in any of the indicated tissue samples of these animals (Figures 4C–4E). These results clearly demonstrate that a single i.n. immunization with live VAS5 not only prevents SARS-CoV-2 infection but also prevents close-contact transmission in hamsters.

Cryo-EM structure of the VAS5 S trimer glycoprotein

To understand the structural impact of the seven-aa deletion on the SARS-CoV-2 spike architecture, we produced VAS5 S protein as a secreted trimer in a mammalian expression system (Figure S3). Highly purified protein with excellent homogenicity was used for cryo-EM data collection. Three-dimensional classification revealed that the VAS5 S trimer adopts two distinct conformational states, corresponding to a closed form with all three receptor binding domains (RBDs) down and an open form with one RBD up for ACE2 binding (Figure S4). We determined cryo-EM reconstructions of the two states at 3.6 Å and 4.2 Å, respectively (Figure S5). The structure of VAS5 S displays the characteristic overall architecture observed for WT SARS-CoV-2 in the closed and open conformations (Figure 5A). Comparison of the VAS5 S protein structure with that of the D614G mutant indicated that the D614G mutation samples the RBD-open conformation more frequently (nearly 95%) and enhances protease cleavage at the furin recognition site.[37–39] In contrast, a seven-aa deletion encompassing the furin cleavage site rendered approximately 90% of VAS5 S in the RBD-closed configuration, similar to structural

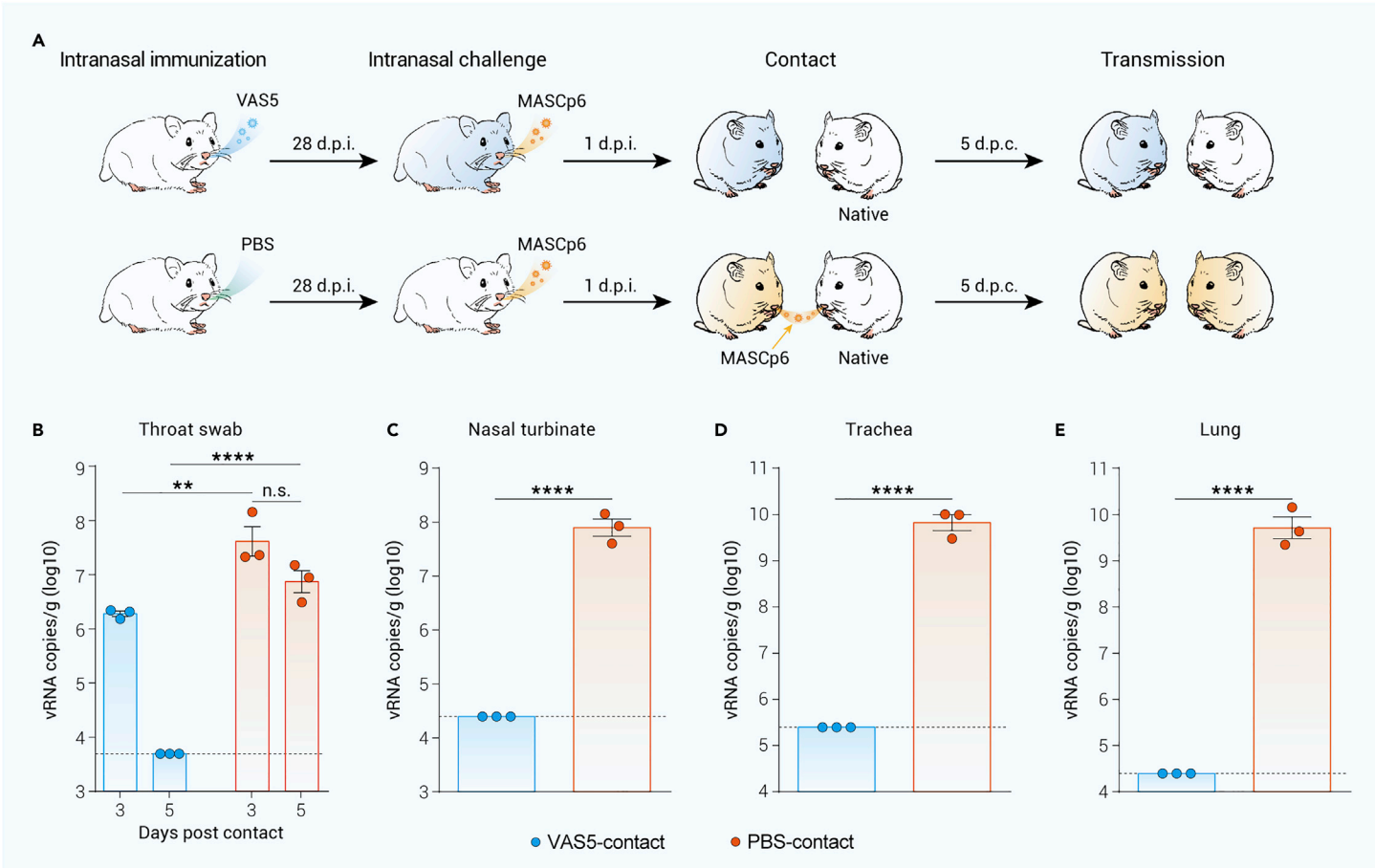

Figure 4. Live-attenuated VAS5 virus can prevent the transmission of SARS-CoV-2 in hamsters (A) Study design of the prevention of contact transmission of SARS-CoV-2 in hamsters. Three immunized animals from the 10^4 PFU-dose group or the PBS group were i.n. challenged with MASCp6 (20,000 PFU/animal). One day post-challenge, each challenged hamster was transferred to a new cage containing one naive hamster as the close contact (A). Viral RNA in throat swabs was detected using RT-qPCR at days 3 and 5 post close contact. (B) The indicated tissues were also collected 5 days after close contact for detection of viral loads using RT-qPCR. (C–E) The indicated tissues were also collected 5 days after challenge for detection of viral loads using RT-qPCR: (C) nasal turbinate; (D) trachea; (E) lung. Data are shown as the mean ± SEM. Statistics were determined by multiple t tests. d.p.c., days post contact; d.p.i., days post infection; n.s., not significant; **p < 0.01; ****p < 0.0001).

observations of SARS-CoV-2-3Q-2P, an advanced vaccine candidate (NVAX-CoV2373).[40] Consistent with this more closed conformation, VAS5 showed remarkably decreased infectivity and fitness in human respiratory epithelial cells and was significantly attenuated in hACE2 mice.

Given that deletions at the S1/S2 junction and distal regions of the S protein can lead to allosteric effects on RBD-open/down disposition, we scrutinized the VAS5 S trimer structure. Deletion of seven-aa shortens the loop that is highly disordered in the WT/variant structures; however, this did not appear to disrupt the S conformation appreciably or perturb the key epitopes on the RBD/N-terminal domain (NTD) (Figure 5B). Perhaps correlated with the expression system used, the VAS5 S trimer did not harbor the hydrophobic pocket or linoleic acid (LA). Previously, LA, a polyunsaturated fatty acid found in the RBD (Figure 5C), was suggested to play a role in potentially stabilizing the RBD-down state by locking the conformation of the S trimer.[41] Unexpectedly, the VAS5 S trimer exhibited a much more compacted architecture in the region formed by the three RBDs, representing a completely locked conformation (Figure 5D), akin to those mediated by LA binding.[40,41] Consequently, the VAS5 S trimer possessed dramatically increased intersubunit interactions spanning up to 5,600 $Å^2$ compared with the closed, but not locked, structure (PDB ID: 6VXX), which exhibited buried areas of 4,600 $Å^2$ between subunits, resulting in enhanced stability for the S trimer in the prefusion conformation (Figures 5E, S6, and S7). Furthermore, analysis of trypsin-mediated S fusogenic conformational rearrangements evaluated by negatively stained EM demonstrated that the VAS5 S trimer presented improved stability in maintaining its prefusion conformation (Figure 5F). Collectively, the results of our structural and biochemical studies reveal traits of VAS5 S, such as a highly stable prefusion configuration without antigenic alterations, which are highly suitable for their potential utility in formulating a vaccine.

Biochemical and immunogenic analysis of the VAS5 S glycoprotein

Despite the locked conformation assumed by the vast majority of particles, binding analysis of the VAS5 S trimer to hACE2 by both biolayer interferometry (BLI) and ELISAs clearly showed binding of the protein to hACE2, indicative of the fact that RBD is dynamic and accessible for receptor binding (Figures 6A and 6B). Compared with the WT, the VAS5 S trimer exhibited slightly decreased binding (Figure 6B). In line with this, a markedly reduced resonance unit signal for the VAS5 S trimer was observed when compared with the WT S trimer under the same concentrations, which is consistent with the previous inference that the WT S trimer presents a higher percentage of open RBDs. There are two pathways proposed for SARS-CoV-2 entry into cells: 1) direct viral fusion at the plasma membrane that is mediated by the host type II transmembrane serine protease TMPRSS2 (called the "early" entry pathway); and 2) hACE2-dependent endocytic entry, which relies on the actions of the lysosomal protease cathepsin (called the "late" entry pathway).[27,42–44] Although Vero cells express very little TMPRSS2, they permit SARS-CoV-2 entry exclusively via the cathepsin-dependent endosomal pathway. S protein cleavage in the variants with mutations/deletions at the S1/S2 cleavage site was largely prevented, leading to a higher percentage of prefusion S trimers in VAS5. Despite slightly decreased binding affinity to hACE2, VAS5 possesses more prefusion S trimers per virion for receptor binding, subsequently entering cells via the cathepsin-dependent endosomal pathway, which might provide possible explanations for the selection mechanisms of these deletions at the S1/S2 cleavage site.

Following structural characterization, the antigenicity of the VAS5 S trimer was assessed and compared with the WT S trimer. Highly purified VAS5 and WT S trimers were tested for neutralizing antibody (NAb) binding by ELISA (Figure 6C). A panel of 43 RBD- and 27 NTD-targeting NAbs that recognize all six and four currently identified groups of epitopes on the RBD and NTD,

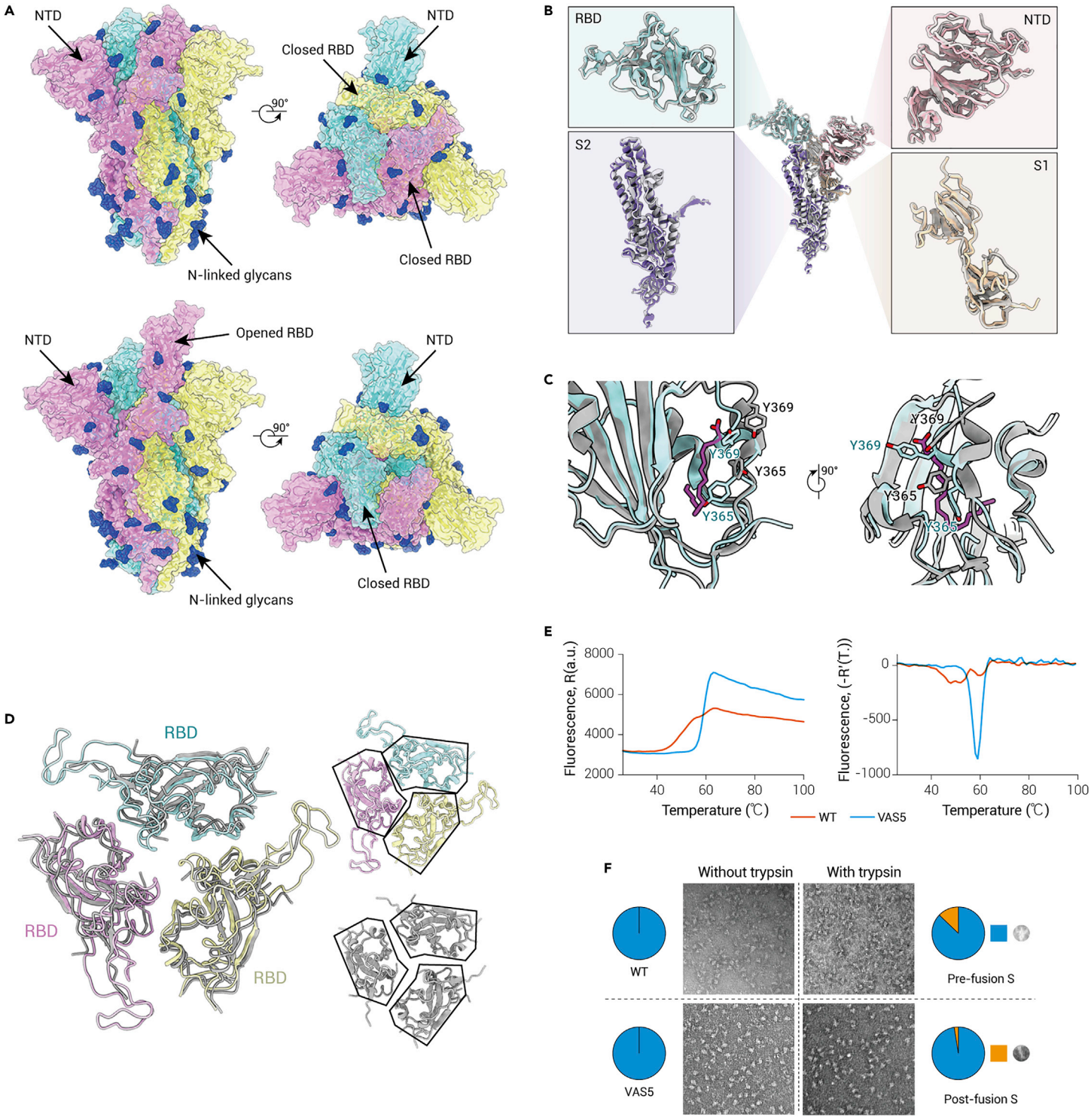

Figure 5. Cryo-EM structure of VAS5 glycoprotein (A) Orthogonal views of VAS5 S trimer with three RBDs in the closed state (upper) and one RBD in the open state (lower). All structures are shown as surfaces with different colors for each S monomer (cyan, pink, and yellow). Glycans are colored dark blue. (B) Superimposition of one monomer of the VAS5 S trimer to the structure of a vaccine immunogen SARS-CoV-2-3Q-2P S trimer (PDB: 7JJI). The enlarged panels show the imposition of four different domains of S. RBD, NTD, S1, and S2 of VAS5 are colored cyan, pink, purple, and wheat, respectively. The monomer of the SARS-CoV-2-3Q-2P S trimer is colored gray. (C) Details of the hydrophobic pocket of RBD. The RBD of the VAS5 S protein is superimposed on the RBD, which harbors a hydrophobic pocket and LA (PDB: 6ZB5). Residues are shown as sticks. RBDs of VAS5 and 6ZB5 are colored cyan and gray, respectively. LA is colored magenta. (D) RBDs in the closed state of VAS5 are superimposed on the previous structure (PDB: 6VXX) and highlighted with black solid lines. RBDs of VAS5 are colored by the same color scheme as in (A), and the structure of 6VXX is colored gray. (E) Stabilities of the purified SARS-CoV-2 S trimer and VAS5 trimer at pH = 7.4 were analyzed by thermofluor assay. We used SYPRO Orange to detect the hydrophobic residues. (F) The conformational state of the WT SARS-CoV-2 S trimer and VAS5 trimer was analyzed using EM of negatively stained samples, and 1.6 μg/mL trypsin was used for the SARS-CoV-2 S trimer and VAS5 trimer. The prefusion and postfusion states are shown at the bottom.

respectively,[45] including several clinically applied therapeutic NAbs or well-studied NAbs.[46–50] Among these RBD-targeting NAbs, two types of NAbs can be classified: 1) only binding to the "up" RBD, and 2) binding to RBDs regardless of their "up" and "down" conformations. The area under the curve (AUC) and the EC_{50} values for each antibody were summarized in two heatmaps corresponding to the VAS5 and WT S trimers, providing the complete antigenic profiles for SARS-CoV-2 (Figures 6C and 6D). Overall, both S trimers exhibited almost identical antigenic (largely similar) properties with group-specific patterns. The antigenic characteristics of the VAS5 S trimer, to some extent, mirror its immunogenicity with NVAX-CoV2373. This

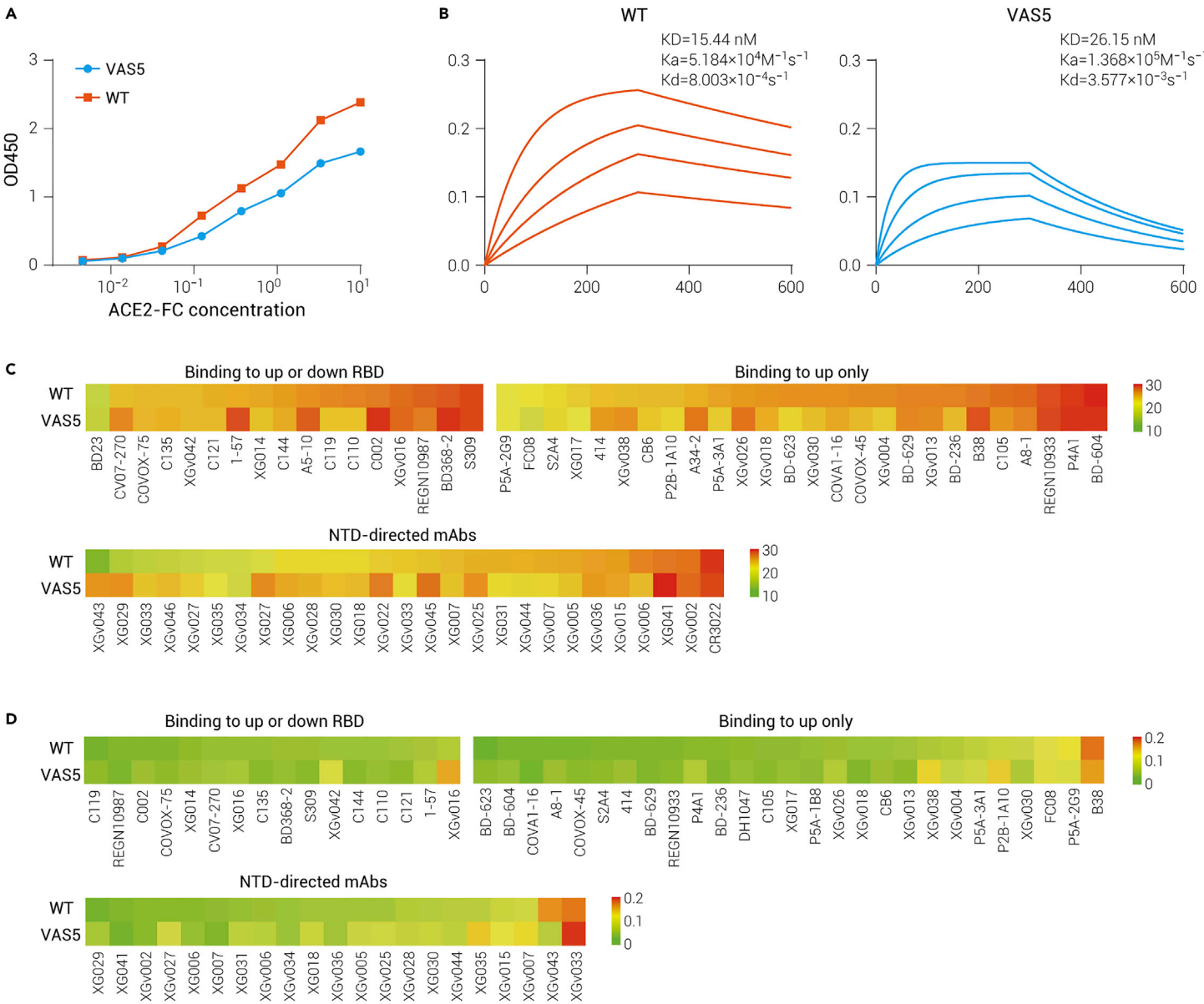

Figure 6. Functional and immunogenic analysis of VAS5 glycoprotein (A) ELISA showing binding to ACE2 by the SARS-CoV-2 spike (red line) and VAS5 spike (blue line). (B) Affinity detection of ACE2 with SARS-CoV-2 spike (red line) and VAS5 spike (blue line) by BLI sensorgram. (C) Heatmap representation of AUC values of the six classes of RBD-targeting mAbs and NTD-targeting mAbs by ELISA against the SARS-CoV-2 S trimer and VAS5 S trimer, respectively, is shown with a color bar indicated on the right. The color gradient for the upper panel indicates AUC values ranging from 10 (green) through 20 (yellow) to 30 (red). (D) Heatmap representation of EC50 of the six classes of RBD-targeting mAbs and NTD-targeting mAbs by ELISAs against the SARS-CoV-2 S trimer and VAS5 S trimer, respectively, is shown with a color bar indicated on the right. The color gradient for the upper panel indicates EC50 values ranging from 0 (green) to 0.1 (yellow) to 0.22 μg/mL (red).

is not surprising, given that both of these S trimers share almost identical structures.[51]

DISCUSSION

Effective vaccines for preventing SARS-CoV-2 infection and transmission are urgently needed. Here, we generated and characterized *in vitro* and *in vivo* attenuation profiles of a Vero-adapted SARS-CoV-2, VAS5 with a seven-aa deletion spanning the PRRA polybasic cleavage motif of the S protein after passaging in Vero cells. Similar observations have been reported where multiple variants bearing furin site deletions emerged in SARS-CoV-2 preparations using Vero E6 cells and in clinical samples.[22,24,25] The frequent detection of these variants suggests that this region is likely to be tolerant of deletions *in vitro*. Interestingly, the seven-aa deletion conferred replication fitness to VAS5 in Vero cells compared with the parental virus. Consistent with the findings from our study, a previous report showed that a SARS-CoV-2 mutant with deletion of PRRA had augmented replication and improved fitness in Vero E6 cells.[52] Our observation, together with previous studies, suggests that there are probably other alternative proteolytic processing pathways in Vero cells that assist SARS-CoV-2 in continuing its life cycle even in the absence of the S1/S2 cleavage site. Furthermore, our cryo-EM data showed that VAS5 possesses more prefusion S trimers per virion for receptor binding,[53] subsequently entering cells via the cathepsin-dependent endosomal pathway, which might provide possible explanations for the selection mechanisms of these deletions at the S1/S2 cleavage site. These observations also underscore the importance of monitoring the genome sequence during the preparation of viral stocks. Notably, our deep sequencing data revealed dynamic population changes during passaging in Vero cells. The variants Δ681-686 and Δ680-686, both of which contained the deletion of the key cleavage motif PRRA, did not become the predominant viral population. Further studies on the functional roles of these deletions in host adaptation are required.

Our data showed that replication of VAS5 was significantly attenuated in human cell lines, human respiratory epithelial air-liquid interface (ALI) culture, and hACE2 mice. Consistent with this finding, a panel of variants containing deletions spanning the PRRA motif or a recombinant ΔPRRA mutant virus were shown to be attenuated in small animal infection models.[54–56] Together, these studies suggest that the polybasic cleavage motif is a virulence determinant in SARS-CoV-2. The underlying mechanism of attenuation is probably that the efficient fusion

process of SARS-CoV-2 is interrupted in the absence of the fusion-like cleavage site, resulting in the production of a large amount of noninfectious viral particles. This speculation is supported by previous studies showing that the polybasic furin-like cleavage site at the S1/S2 junction conferred efficient S-protein-mediated cell-cell fusion and entry into human lung cells.[21,44] Wrobel et al. also found that cleavage at the furin cleavage site decreases the overall stability of the SARS-CoV-2 S protein and facilitates the adoption of the open conformation required for the S protein to bind to hACE2.[57] In previous WT/stably modified S cryo-EM structures, approximately 50% of the S trimers were in the open conformation,[11,15] in contrast to our observation of ~90% in the closed conformation. This result might be caused by the deletion at the S1/S2 cleavage site, leading to allosteric effects on RBD-open/down disposition. The more closed conformation of the VAS5 S trimer may contribute to its remarkably decreased infectivity and fitness *in vitro* and *in vivo*. Notably, all the attenuated variants or the recombinant mutant virus carry motif deletions of different lengths but exhibit different replication capacities in human cell lines. Further studies are needed to clarify the biological significance of amino acids around the cleavage motif in COVID-19.

Deletions in the S protein are supposed to alter the conformation of the spike on the virion particle surface, resulting in a reduction in neutralizing antibodies against circulating strains. A previous study reported that the loss of the furin cleavage site resulted in a reduction in the capacity of COVID-19 serum neutralization,[54] suggesting that loss of the furin cleavage site left more intact spike molecules on the virion surface that would require more neutralizing antibodies. To our surprise, both inactivated VAS5 and live-attenuated VAS5 still provided sufficient protection against viral challenge in mice and hamsters. Consistent with our findings, hamsters infected with SARS-CoV-2 bearing the deletion of the furin cleavage site showed resistance to subsequent infection with the parental strain or even the currently emerging SARS-CoV-2 variants.[54–56] Despite no appreciable alterations in the overall structure, our cryo-EM structure data showed that the VAS5 S trimer exhibited a highly stable and fully locked prefusion conformation, most similar to the structure of a vaccine immunogen SARS-CoV-2-3Q-2P S trimer. In line with this, antigenic profiling by assessing reactions with currently available NAbs further confirmed that the VAS5 S trimer presents an enhanced close antigenic mimic of the native S trimer. Furthermore, in contrast to the observation of the D614G mutation sampling the RBD-open conformation more frequently (nearly 95%), thereby enhancing protease cleavage at the furin recognition site,[37–39] the seven-aa deletion encompassing the furin cleavage site rendered approximately 80% of VAS5 S trimer particles in the RBD-closed configuration, similar to structural observations of SARS-CoV-2-3Q-2P, an advanced vaccine candidate (NVAX-CoV2373), with the closed form predominating.[40,58]

More importantly, two doses of i.m. immunization with inactivated VAS5 or a single dose of i.n. immunization with live VAS5 infection confers protection in either mice or hamsters. These results have significant implications. First, VAS5 can be further developed as an inactivated vaccine to replace the original version.[33] The use of VAS5 will not only reduce the risk of infection during the manufacturing process before inactivation but also increase the protection efficacy due to the increased immunogenicity conferred by the improved antigen. Second, VAS5 can be further developed as a live attenuated vaccine (LAV) that only requires a single injection. LAV mimics natural infection, thus activating all branches of the host immune system. Moreover, VAS5 contains the most protective T cell epitopes outside the S protein.[59,60] Upon i.n. injection with VAS5, humoral and cellular immune responses, as well as mucosal immunity, could be stimulated by this live-attenuated vaccine. Recently, mucosal IgA secretion has been reported to enhance SARS-CoV-2 neutralization,[61] and i.n. delivery of several adenovirus-vectored vaccine candidates were shown to confer protection in mice.[62,63] Finally, an ideal COVID-19 vaccine is supposed to prevent SARS-CoV-2 transmission. However, current vaccines have shown limited efficacy in preventing transmission.[64] Our study showed that a single i.n. immunization with live VAS5 also prevents close-contact transmission in hamsters. These encouraging results warrant further validation in clinical trials.

There are several limitations in this study. First, because safety is the most concerning issue for all LAV candidates, more safety data are warranted to fully evaluate the attenuation phenotypes of VAS5 in other available animal models. Second, the cross-protection against the newly emerged Variants of Concern (VOC) requires further validation. Finally, the magnitude and durability of the mucosal immune response induced by VAS5 should be further evaluated in animal models and clinical trials.

Together, our study identified a Vero-adapted SARS-CoV-2 strain VAS5 carrying a specific deletion in the furin-like cleavage site, which displays replicative fitness in Vero cells but attenuation phenotypes in human cells, organoids, and mice. More importantly, VAS5 exhibits increased immunogenicity, and a single immunization confers protection against SARS-CoV-2 infection and transmission in mice and hamsters. Further clinical development as an alternative COVID-19 vaccine candidate is warranted in the future.

REFERENCES

1. Wu, F., Zhao, S., Yu, B., et al. (2020). A new coronavirus associated with human respiratory disease in China. Nature ***579***, 265–269.
2. Zhou, P., Yang, X.L., Wang, X.G., et al. (2020). A pneumonia outbreak associated with a new coronavirus of probable bat origin. Nature ***579***, 270–273.
3. Zhu, N., Zhang, D., Wang, W., et al. (2020). A novel coronavirus from patients with pneumonia in China, 2019. N. Engl. J. Med. ***382***, 727–733.
4. Huang, C., Wang, Y., Li, X., et al. (2020). Clinical features of patients infected with 2019 novel coronavirus in Wuhan, China. Lancet ***395***, 497–506.
5. Guan, W.J., Ni, Z.Y., Hu, Y., et al. (2020). Clinical characteristics of coronavirus disease 2019 in China. N. Engl. J. Med. ***382***, 1708–1720.
6. Zhou, F., Yu, T., Du, R., et al. (2020). Clinical course and risk factors for mortality of adult inpatients with COVID-19 in Wuhan, China: a retrospective cohort study. Lancet ***395***, 1054–1062.
7. Hao, X., Cheng, S., Wu, D., et al. (2020). Reconstruction of the full transmission dynamics of COVID-19 in Wuhan. Nature ***584***, 420–424.
8. Li, Q., Guan, X., Wu, P., et al. (2020). Early transmission dynamics in Wuhan, China, of novel coronavirus-infected pneumonia. N. Engl. J. Med. ***382***, 1199–1207.
9. Liu, Y., and Rocklov, J. (2021). The reproductive number of the Delta variant of SARS-CoV-2 is far higher compared to the ancestral SARS-CoV-2 virus. J. Trav. Med. ***28***, 1–3.
10. Letko, M., Seifert, S.N., Olival, K.J., et al. (2020). Bat-borne virus diversity, spillover and emergence. Nat. Rev. Microbiol. ***18***, 461–471.
11. Walls, A.C., Park, Y.J., Tortorici, M.A., et al. (2020). Structure, function, and antigenicity of the SARS-CoV-2 spike glycoprotein. Cell ***181***, 281–292.e6.
12. Millet, J.K., and Whittaker, G.R. (2015). Host cell proteases: critical determinants of coronavirus tropism and pathogenesis. Virus Res. ***202***, 120–134.
13. Andersen, K.G., Rambaut, A., Lipkin, W.I., et al. (2020). The proximal origin of SARS-CoV-2. Nat. Med. ***26***, 450–452.
14. Coutard, B., Valle, C., de Lamballerie, X., et al. (2020). The spike glycoprotein of the new coronavirus 2019-nCoV contains a furin-like cleavage site absent in CoV of the same clade. Antivir. Res. ***176***, 104742.
15. Wrapp, D., Wang, N., Corbett, K.S., et al. (2020). Cryo-EM structure of the 2019-nCoV spike in the prefusion conformation. Science ***367***, 1260–1263.
16. Braun, E., and Sauter, D. (2019). Furin-mediated protein processing in infectious diseases and cancer. Clin. Transl. Immunol. ***8***, e1073.
17. Chen, J., Lee, K.H., Steinhauer, D.A., et al. (1998). Structure of the hemagglutinin precursor cleavage site, a determinant of influenza pathogenicity and the origin of the labile conformation. Cell ***95***, 409–417.
18. Luczo, J.M., Stambas, J., Durr, P.A., et al. (2015). Molecular pathogenesis of H5 highly pathogenic avian influenza: the role of the haemagglutinin cleavage site motif. Rev. Med. Virol. ***25***, 406–430.
19. Zhou, H., Chen, X., Hu, T., et al. (2020). A novel bat coronavirus closely related to SARS-CoV-2 contains natural insertions at the S1/S2 cleavage site of the spike protein. Curr. Biol. ***30***, 2196–2203.e2193.
20. Follis, K.E., York, J., and Nunberg, J.H. (2006). Furin cleavage of the SARS coronavirus spike glycoprotein enhances cell-cell fusion but does not affect virion entry. Virology ***350***, 358–369.
21. Hoffmann, M., Kleine-Weber, H., and Pohlmann, S. (2020). A multibasic cleavage site in the spike protein of SARS-CoV-2 is essential for infection of human lung cells. Mol. Cell. ***78***, 779–784.e775.
22. Davidson, A.D., Williamson, M.K., Lewis, S., et al. (2020). Characterisation of the transcriptome and proteome of SARS-CoV-2 reveals a cell passage induced in-frame deletion of the furin-like cleavage site from the spike glycoprotein. Genome Med. ***12***, 68.
23. Lau, S.Y., Wang, P., Mok, B.W., et al. (2020). Attenuated SARS-CoV-2 variants with deletions at the S1/S2 junction. Emerg. Microbes Infect. ***9***, 837–842.
24. Liu, Z., Zheng, H., Lin, H., et al. (2020). Identification of common deletions in the spike protein of severe acute respiratory syndrome coronavirus 2. J. Virol. ***94***, e00790-20.
25. Wong, Y.C., Lau, S.Y., Wang To, K.K., et al. (2021). Natural transmission of bat-like severe acute respiratory syndrome coronavirus 2 without proline-arginine-arginine-alanine variants in coronavirus disease 2019 patients. Clin. Infect. Dis. ***73***, e437–e444.
26. Pohl, M.O., Busnadiego, I., Kufner, V., et al. (2021). SARS-CoV-2 variants reveal features critical for replication in primary human cells. PLoS. Biol. ***19***, e3001006.
27. Sasaki, M., Uemura, K., Sato, A., et al. (2021). SARS-CoV-2 variants with mutations at the S1/S2 cleavage site are generated in vitro during propagation in TMPRSS2-deficient cells. PLoS. Pathog. ***17***, e1009233.
28. Polack, F.P., Thomas, S.J., Kitchin, N., et al. (2020). Safety and efficacy of the BNT162b2 mRNA Covid-19 vaccine. N. Engl. J. Med. ***383***, 2603–2615.

29. Voysey, M., Clemens, S.A.C., Madhi, S.A., et al. (2021). Safety and efficacy of the ChAdOx1 nCoV-19 vaccine (AZD1222) against SARS-CoV-2: an interim analysis of four randomised controlled trials in Brazil, South Africa, and the UK. Lancet ***397***, 99–111.
30. Wu, Z., Hu, Y., Xu, M., et al. (2021). Safety, tolerability, and immunogenicity of an inactivated SARS-CoV-2 vaccine (CoronaVac) in healthy adults aged 60 years and older: a randomised, double-blind, placebo-controlled, phase 1/2 clinical trial. Lancet Infect. Dis. ***21***, 803–812.
31. Xia, S., Zhang, Y., Wang, Y., et al. (2021). Safety and immunogenicity of an inactivated SARS-CoV-2 vaccine, BBIBP-CorV: a randomised, double-blind, placebo-controlled, phase 1/2 trial. Lancet Infect. Dis. ***21***, 39–51.
32. Zhu, F.C., Li, Y.H., Guan, X.H., et al. (2020). Safety, tolerability, and immunogenicity of a recombinant adenovirus type-5 vectored COVID-19 vaccine: a dose-escalation, open-label, non-randomised, first-in-human trial. Lancet ***395***, 1845–1854.
33. Gao, Q., Bao, L., Mao, H., et al. (2020). Development of an inactivated vaccine candidate for SARS-CoV-2. Science ***369***, 77–81.
34. Zhang, N.N., Li, X.F., Deng, Y.Q., et al. (2020). A thermostable mRNA vaccine against COVID-19. Cell ***182***, 1271–1283.e1216.
35. Chan, J.F., Zhang, A.J., Yuan, S., et al. (2020). Simulation of the clinical and pathological manifestations of coronavirus disease 2019 (COVID-19) in a golden syrian hamster model: implications for disease pathogenesis and transmissibility. Clin. Infect. Dis. ***71***, 2428–2446.
36. Sia, S.F., Yan, L.M., Chin, A.W.H., et al. (2020). Pathogenesis and transmission of SARS-CoV-2 in golden hamsters. Nature ***583***, 834–838.
37. Gobeil, S.M., Janowska, K., McDowell, S., et al. (2021). D614G mutation alters SARS-CoV-2 spike conformation and enhances protease cleavage at the S1/S2 junction. Cell. Rep. ***34***, 108630.
38. Yurkovetskiy, L., Wang, X., Pascal, K.E., et al. (2020). Structural and functional analysis of the D614G SARS-CoV-2 spike protein variant. Cell ***183***, 739–751.e738.
39. Zhang, J., Cai, Y., Xiao, T., et al. (2021). Structural impact on SARS-CoV-2 spike protein by D614G substitution. Science ***372***, 525–530.
40. Bangaru, S., Ozorowski, G., Turner, H.L., et al. (2020). Structural analysis of full-length SARS-CoV-2 spike protein from an advanced vaccine candidate. Science ***370***, 1089–1094.
41. Toelzer, C., Gupta, K., Yadav, S.K.N., et al. (2020). Free fatty acid binding pocket in the locked structure of SARS-CoV-2 spike protein. Science ***370***, 725–730.
42. Shang, J., Wan, Y., Luo, C., et al. (2020). Cell entry mechanisms of SARS-CoV-2. Proc. Natl. Acad. Sci. U S A. ***117***, 11727–11734.
43. Ou, X., Liu, Y., Lei, X., et al. (2020). Characterization of spike glycoprotein of SARS-CoV-2 on virus entry and its immune cross-reactivity with SARS-CoV. Nat. Commun. ***11***, 1620.
44. Hoffmann, M., Kleine-Weber, H., Schroeder, S., et al. (2020). SARS-CoV-2 cell entry depends on ACE2 and TMPRSS2 and is blocked by a clinically proven protease inhibitor. Cell ***181***, 271–280.e278.
45. Wang, K., Cao, Y., Zhou, Y., et al. (2021). A third dose of inactivated vaccine augments the potency, breadth, and duration of anamnestic responses against SARS-CoV-2. Preprint at medRxiv. https://doi.org/10.1101/2021.09.02.21261735.
46. Sun, Y., Wang, L., Feng, R., et al. (2021). Structure-based development of three- and four-antibody cocktails against SARS-CoV-2 via multiple mechanisms. Cell. Res. ***31***, 597–600.
47. Zhu, L., Deng, Y.Q., Zhang, R.R., et al. (2021). Double lock of a potent human therapeutic monoclonal antibody against SARS-CoV-2. Natl. Sci. Rev. ***8***, nwaa297.
48. Zhang, L., Cao, L., Gao, X.S., et al. (2021). A proof of concept for neutralizing antibody-guided vaccine design against SARS-CoV-2. Natl. Sci. Rev. ***8***, nwab053.
49. Yao, H., Sun, Y., Deng, Y.Q., et al. (2021). Rational development of a human antibody cocktail that deploys multiple functions to confer Pan-SARS-CoVs protection. Cell. Res. ***31***, 25–36.
50. Lv, Z., Deng, Y.Q., Ye, Q., et al. (2020). Structural basis for neutralization of SARS-CoV-2 and SARS-CoV by a potent therapeutic antibody. Science ***369***, 1505–1509.
51. Keech, C., Albert, G., Cho, I., et al. (2020). Phase 1-2 trial of a SARS-CoV-2 recombinant spike protein nanoparticle vaccine. N. Engl. J. Med. ***383***, 2320–2332.
52. Johnson, B.A., Xie, X., Kalveram, B., et al. (2020). Furin cleavage site is key to SARS-CoV-2 pathogenesis. Preprint at bioRxiv. https://doi.org/10.1101/2020.08.26.268854.
53. Tai, L., Zhu, G., Yang, M., et al. (2021). Nanometer resolution in situ structure of SARS-CoV-2 post-fusion spike. Proc. Natl. Acad. Sci. U S A. ***118***, e2112703118.
54. Johnson, B.A., Xie, X., Bailey, A.L., et al. (2021). Loss of furin cleavage site attenuates SARS-CoV-2 pathogenesis. Nature ***591***, 293–299.
55. Sasaki, M., Toba, S., Itakura, Y., et al. (2021). SARS-CoV-2 bearing a mutation at the S1/S2 cleavage site exhibits attenuated virulence and confers protective immunity. mBio ***12***, e0141521.
56. Wang, P., Lau, S.Y., Deng, S., et al. (2021). Characterization of an attenuated SARS-CoV-2 variant with a deletion at the S1/S2 junction of the spike protein. Nat. Commun. ***12***, 2790.
57. Wrobel, A.G., Benton, D.J., Xu, P., et al. (2020). SARS-CoV-2 and bat RaTG13 spike glycoprotein structures inform on virus evolution and furin-cleavage effects. Nat. Struct. Mol. Biol. ***27***, 763–767.
58. Gupta, K., Toelzer, C., Williamson, M.K., et al. (2021). Structural basis for cell-type specific evolution of viral fitness by SARS-CoV-2. Preprint at bioRxiv. https://doi.org/10.1101/2021.05.11.443384.
59. Grifoni, A., Sidney, J., Zhang, Y., et al. (2020). A sequence homology and bioinformatic approach can predict candidate targets for immune responses to SARS-CoV-2. Cell. Host. Microbe ***27***, 671–680.e672.
60. Mateus, J., Grifoni, A., Tarke, A., et al. (2020). Selective and cross-reactive SARS-CoV-2 T cell epitopes in unexposed humans. Science ***370***, 89–94.
61. Wang, Z., Lorenzi, J.C.C., Muecksch, F., et al. (2021). Enhanced SARS-CoV-2 neutralization by dimeric IgA. Sci. Transl. Med. ***13***, eabf1555.
62. Hassan, A.O., Kafai, N.M., Dmitriev, I.P., et al. (2020). A single-dose intranasal Chad vaccine protects upper and lower respiratory tracts against SARS-CoV-2. Cell ***183***, 169–184.e113.
63. Hassan, A.O., Shrihari, S., Gorman, M.J., et al. (2021). An intranasal vaccine durably protects against SARS-CoV-2 variants in mice. Cell. Rep. ***36***, 109452.
64. Ioannou, P., Karakonstantis, S., Astrinaki, E., et al. (2021). Transmission of SARS-CoV-2 variant B.1.1.7 among vaccinated health care workers. Infect. Dis. (Lond) ***53***, 876–879.

ACKNOWLEDGMENTS

We thank Drs. Changfa Fan, Liang Li, and Guan Yang for critical material and helpful discussion. This work was supported by the National Key Research and Development Program of China (No. 2020YFC0840900, 2018YFA0900801 and 2020YFA0707500), the Strategic Priority Research Program (XDB29010000, XDB37030000), CAS (YSBR-010), the Emergency Key Program of Guangzhou Laboratory (No. EKPG21-09), the Beijing Municipal Science and Technology Project (No. Z201100001020004, Z201100005420017), and the National Natural Science Foundation of China (No. 82171820, No. 12034006, and No. 81921005). C.-F.Q. was supported by the National Science Fund for Distinguished Young Scholars (81925025), the Innovative Research Group (81621005) from the NSFC, and the Innovation Fund for Medical Sciences (2019-I2 M-5-049) from the Chinese Academy of Medical Sciences.

AUTHOR CONTRIBUTIONS

C.F.Q. and X.W. conceived and supervised the study. X.F.L., Q.C., Q.Y., and Y.Q.D were responsible for conducting experiments in Biosafety Level 3 facilities. Z.C., Z.J., and K.F. expressed and purified all recombinant proteins. Z.C., Z.J., and K.F. performed the BLI assay and the Termofulor assay. L.W. and L.C. performed the structural study. Y. G. performed the sequencing experiments. H.F. and S.Q. performed sequencing data analysis. H.Y.Q. and N.N.Z. performed the RNA ISH assay; R.R.Z. carried out RT-qPCR; Y.P.X. and C.Z. performed immunofluorescent staining; X.F.L., Z.C., H.F., Y.C., X.W., and C.F.Q. analyzed the data. X.F.L., X.W., and C.F.Q. wrote the initial manuscript. All authors reviewed and approved the manuscript.

DECLARATION OF INTERESTS

C.F.Q. and X.F.L. have filed a patent relevant to the use of VAS5 as vaccine candidates.

SUPPLEMENTAL INFORMATION

Supplemental information can be found online at https://doi.org/10.1016/j.xinn.2022.100221.

LEAD CONTACT WEBSITE

https://publons.com/researcher/1354271/cheng-feng-qin.